

Production and Characterization of Activated Biochar from Cattail Plant for Methylene Blue Adsorption

Mrs. Mahasowmiya S

Assistant Professor

Department of Chemical Engineering, St. Michael College of Engineering & Technology, Kalaiyarkoil.

Sudhantira Pandiyan S, Balamurugan P,

Deepak K, Mohanraj K

St. Michael College of Engineering and Technology, Kalaiyarkoil.

Abstract - This study focuses on producing activated biochar from cattail plant via pyrolysis and chemical activation with KOH. The biochar was characterized and tested for methylene blue (MB) adsorption. Results showed that pyrolysis temperature significantly affects biochar yield. The activated biochar (KAC) was characterized by the FTIR, UV spectroscopy, SEM analysis Methods.

1. Introduction

Cattail plant is a widespread aquatic weed, poses ecological and environmental challenges in water bodies. Utilizing this invasive biomass for value-added products like biochar can mitigate its impact and contribute to wastewater treatment. Biochar, a carbon-rich material produced via pyrolysis, has gained attention for its adsorption capabilities in removing pollutants like dyes from wastewater. This study explores the production of activated biochar from cattail plant via pyrolysis and chemical activation with KOH, evaluating its potential for methylene blue (MB) adsorption.

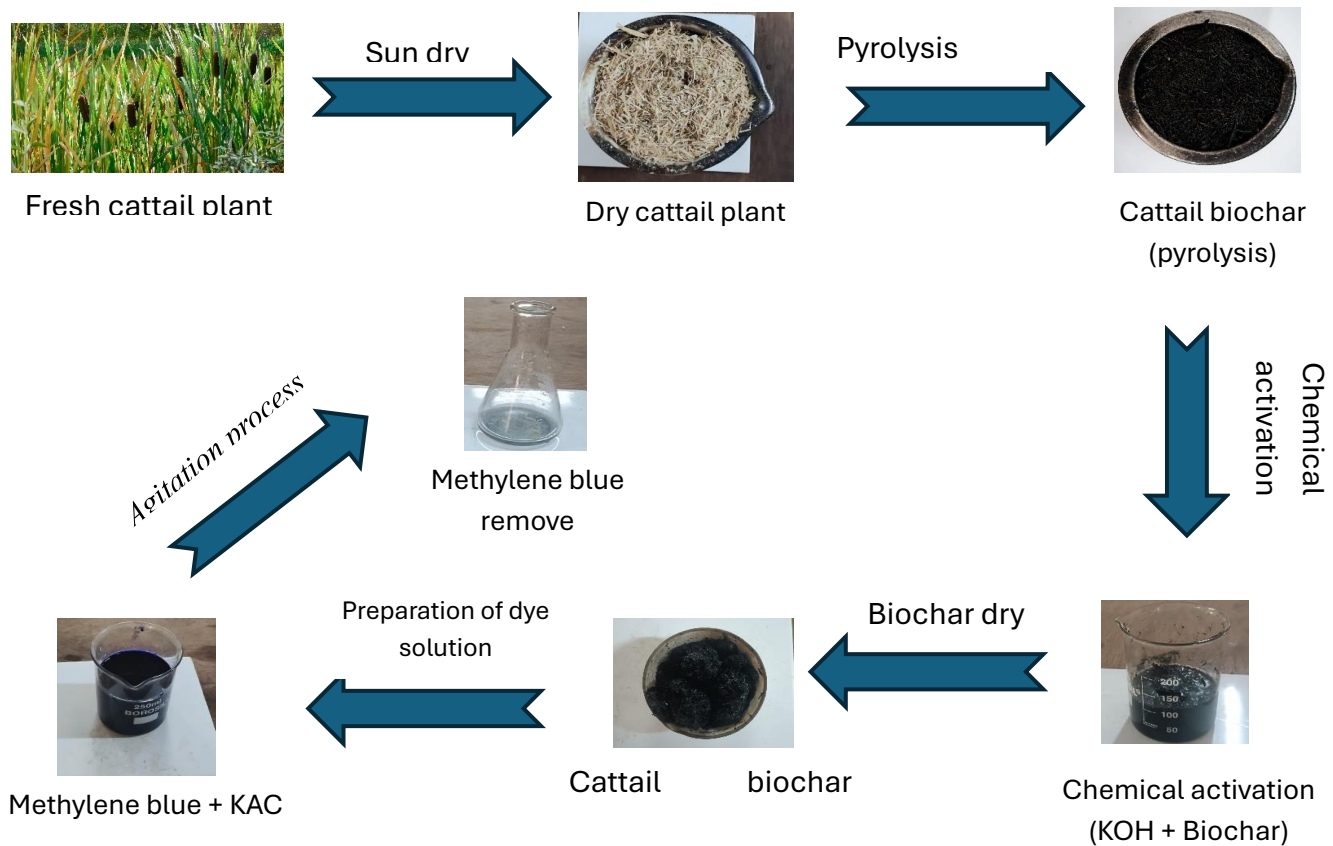
2. Materials And Methods

2.1 Production of biochar from cattail plant

The cattail plant was collected from Kalaiyarkoil. The cattail plant was washed and sun-dried for 20 days. The dry biomass was ground and sieved to obtain uniform particle size. The dried biomass was subjected to pyrolysis at 500°C at a heating rate of 20°C/min in a muffle furnace.

2.2 Preparation of activated biochar from cattail plant

The chemical activation process with potassium hydroxide (KOH) was conducted as follows: the biochar produced was soaked in potassium hydroxide (KOH) solution (3M) with a char/KOH impregnation ratio of 1:20 (weight: volume). After impregnating for 12 hours, the obtained biochar was washed with 0.1M HCl until the pH of the washing solution reached 6-7. Then the biochar was dried at 60°C for 6 hours in an oven and recorded as KAC.



3. Determination of the point of zero charge (pHpzc) of the Material

A series of 0.1 M NaCl solutions with initial pH values (pHi) ranging from 1 to 10 was prepared. The pH was adjusted using 0.1 M HCl or 0.1 M NaOH. Ten 100 mL Erlenmeyer flasks were set up, each containing 0.05 g of KAC material. Subsequently, 100 mL of NaCl solution at the corresponding initial pH was added to each flask. The mixtures were left undisturbed for 48 hours to reach equilibrium, after which the suspensions were filtered, and the final pH (pHf) of each solution was measured. The pH difference (ΔpH) was calculated using the equation $\Delta\text{pH} = \text{pHf} - \text{pHi}$. A graph of ΔpH versus pHi was plotted, and the point at which the curve intersects the x-axis (where $\Delta\text{pH} = 0$) was identified as the point of zero charge (pHpzc) of the material.

4. Study of Adsorption Process

The adsorption experiments were carried out in 150 mL conical flasks containing 20 mL of methylene blue (MB) solution with an initial concentration of 150 mg/L. The experimental conditions were optimized by varying the adsorbent dosage from 1 to 3 g/L, pH from 6 to 12, and temperature from 288 to 308 K. The flasks were agitated in a temperature-controlled shaker at 150 rpm for 240 minutes. After completion of the adsorption process, the samples were filtered using filter paper. The residual concentration of MB was determined using a UV-Visible spectrophotometer at a wavelength of 664 nm. The removal efficiency of MB (R) was calculated using Eq.(1).

$$R = \frac{(C_0 - C_e)}{C_0} \times 100 \quad (1)$$

Where, R is the adsorption efficiency (%), C_0 is the initial concentration of the solution (mg L^{-1}), C_e is the equilibrium concentration of the solution (mg L^{-1}).

5. Adsorption isotherm

The adsorption isotherm was used to describe the relationship between the adsorption capacity and the equilibrium concentration of the adsorbate. A 0.03 g adsorbent was added into a 100 mL conical flask containing 20 mL of MB solution with concentrations

ranging from 5 to 200 mg/L. The mixture was agitated in a temperature-controlled shaker at a speed of 150 rpm under three different temperatures (288 K, 298 K, and 318 K) for 240 min. After the adsorption process, the samples were filtered using filter paper. The absorbance of the MB solution was measured at 664 nm using a UV–Visible spectrophotometer. The Langmuir and Freundlich isotherm models were applied to evaluate the isotherm parameters using Eqs. (2) and (3).

$$\frac{C_e}{q_e} = \frac{1}{K_L q_m} + \frac{C_e}{q_m} \quad (2)$$

$$\ln q_e = \frac{1}{n} \ln C_e - \ln K_F \quad (3)$$

where C_e and q_e represented the equilibrium concentration(mg/L) of MB solution and equilibrium adsorption capacity (mg/g), respectively, q_m was the maximum adsorption capacity of MB (mg/g), K_L was the Langmuir constant (L/mg) and K_F was Freundlich constant (L/mg).

6. RESULTS

6.1 Biochar Yield (%)

Figure 1 shows that increasing the pyrolysis temperatures significantly reduces the biochar yield due to the enhanced decomposition of cellulose, hemicellulose, and lignin, as moisture and volatiles compounds are released. This process produces a stable carbonaceous material with ideal textural properties for pollutant adsorption. The biochar yield was evaluated at different pyrolysis temperatures ranging from 300°C to 700°C. The yield percentage was calculated using the ratio of the final biochar weight to the initial biomass weight. The results showed that the yield decreased progressively with increasing temperature, where 85% yield was obtained at 300°C, which reduced to 75%, 60%, 40%, and 30% at 400°C, 500°C, 600°C, and 700°C, respectively. This decreasing trend is attributed to the enhanced thermal decomposition of biomass components such as hemicellulose, cellulose, and lignin at higher temperatures, leading to the release of volatile compounds and reduction in solid residue. At lower temperatures, incomplete carbonization retains more mass, resulting in higher yield, whereas at elevated temperatures, extensive devolatilization and carbon loss occur, thereby reducing the overall biochar yield. These results clearly indicate that temperature plays a crucial role in determining the yield and properties of biochar.

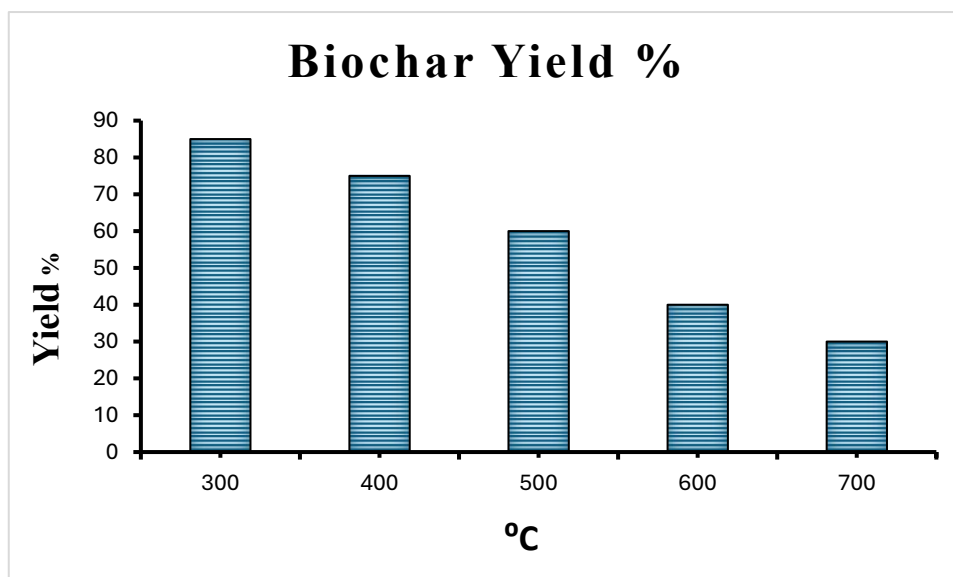


Figure 1. Cattail plant biochar yields (%) at different pyrolysis temperatures.

6.2 MB Removal %

The removal efficiency of methylene blue was investigated at different solution volumes ranging from 10 mL to 100 mL under constant adsorption conditions. The percentage removal was calculated based on the initial and final dye concentrations. The results indicated that the removal efficiency decreased with increasing solution volume, where a maximum removal of 80% was observed at 10 mL, which gradually declined to 60%, 56%, 55%, 48%, 45%, and 25% at 20 mL, 30 mL, 40 mL, 50 mL, 60 mL, and 100 mL, respectively. This reduction in removal efficiency at higher volumes can be attributed to the fixed amount of adsorbent used, which becomes insufficient to effectively interact with the increased number of dye molecules present in larger solution volumes. Consequently, the availability of active adsorption sites decreases relative to the dye concentration, leading to lower removal efficiency. These findings suggest that solution volume is a critical parameter influencing adsorption performance.

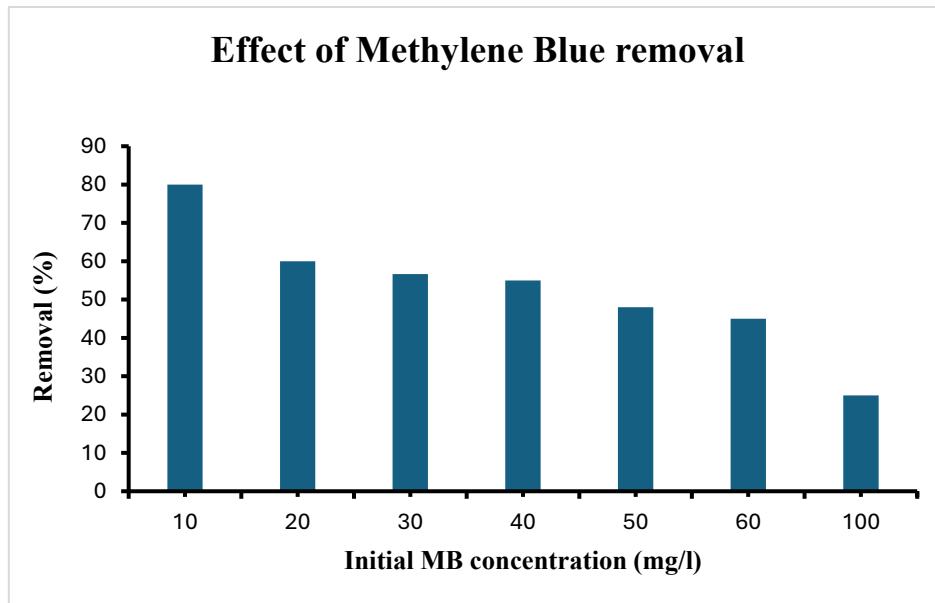


Figure 2. Effect of initial MB concentration on the adsorption efficiency of KAC obtained from cattail plant

6.3 Point of zero charge (pHpzc)

The point of zero charge (pHpzc) of the KAC material is presented in Fig. 7. Based on the experimental results, the pHpzc of KAC was determined to be approximately 7. This value is in close agreement with previously reported studies on activated carbon materials, which typically exhibit pHpzc values in the neutral range. The pHpzc value indicates that the surface of KAC carries a positive charge when the solution pH is lower than 7, whereas the surface becomes negatively charged when the solution pH exceeds this value. This surface charge behavior plays a crucial role in governing the adsorption interactions between KAC and ionic species in aqueous solutions, particularly enhancing the adsorption of cationic dyes such as methylene blue at pH values above the pHpzc.

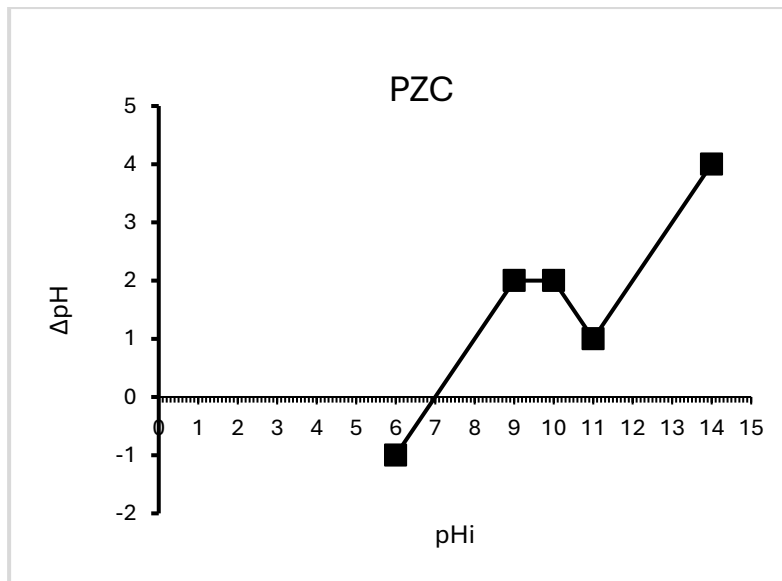


Figure 3. Determination of the point of zero charge (pHpzc) of KAC.

6.4 Adsorption isotherm models

6.4.1 Langmuir isotherm model. The adsorption isotherm study was carried out to evaluate the interaction between the adsorbate and the adsorbent. The experimental data were analyzed using the Langmuir Adsorption Isotherm model, and the corresponding linear plot is presented in Fig. X. The Langmuir model showed a good linear fit with a correlation coefficient (R^2) value of 0.9386, indicating that the adsorption process follows a monolayer adsorption mechanism on a homogeneous surface. The maximum adsorption capacity (q_{max}) was determined to be 10.60 mg/g, demonstrating the effectiveness of the adsorbent. Furthermore, the dimensionless separation factor (RL) was found to be in the range of $0 < RL < 1$, confirming that the adsorption process is favorable and spontaneous.

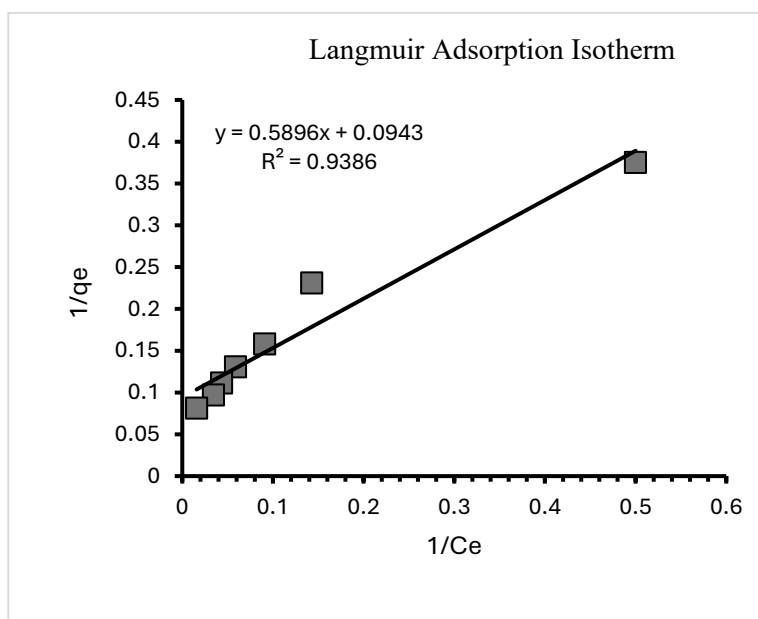


Figure 3. Langmuir adsorption isotherm.

6.4.2 Freundlich isotherm model.

The adsorption equilibrium data were further analyzed using the Freundlich Isotherm model to describe the adsorption behavior on a heterogeneous surface. The corresponding linear plot of $\log q_e$ versus $\log C_e$ is presented in Fig. X. The Freundlich model exhibited a strong linear relationship with a high correlation coefficient (R^2) value of 0.9775, indicating a good fit to the experimental data. This suggests that the adsorption process occurs on a heterogeneous surface with multilayer adsorption. From the linear regression equation ($y = 0.4748x + 0.2844$), the Freundlich constants were determined, where the slope ($1/n$) was found to be 0.4748 and the intercept ($\log KF$) was 0.2844. The value of $1/n$ less than 1 indicates that the adsorption process is favorable. Overall, the results demonstrate that the Freundlich model effectively describes the adsorption behavior of the system, suggesting surface heterogeneity and multilayer adsorption.

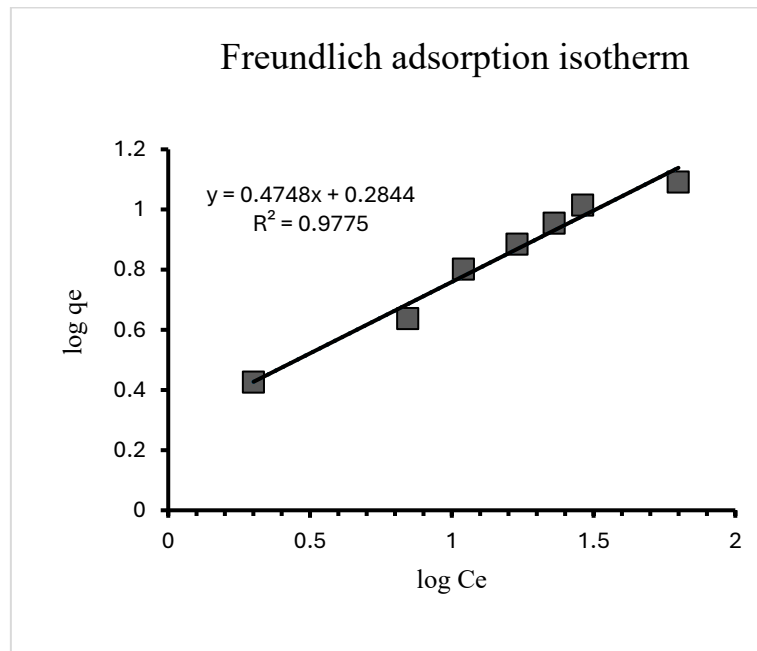


Figure 4. Freundlich adsorption isotherm.

7. Characterization Techniques

7.1 FTIR Analysis. The Fourier Transform Infrared Spectroscopy spectra of biochar before and after chemical activation are presented in Fig.1 and Fig.2, and the corresponding functional groups are summarized in Table X. The pyrolyzed biochar exhibited characteristic peaks at 3317.32 cm^{-1} ($-\text{OH}$), 1575.54 cm^{-1} ($\text{C}=\text{C}$), 1409.50 cm^{-1} ($\text{C}-\text{H}$), and 1110.92 cm^{-1} ($\text{C}-\text{O}$), indicating the presence of hydroxyl, aromatic, and oxygen-containing functional groups. After chemical activation, a noticeable shift and increase in peak intensity were observed, particularly in the hydroxyl group ($3317 \rightarrow 3346 \text{ cm}^{-1}$), suggesting an enhancement in surface functional groups. The aromatic $\text{C}=\text{C}$ peak showed a slight shift ($1575 \rightarrow 1569 \text{ cm}^{-1}$), while the $\text{C}-\text{O}$ stretching region became broader, indicating the increased presence of oxygen-containing groups. These changes confirm that chemical activation significantly modifies the surface chemistry of the biochar by introducing additional functional groups and increasing the number of active sites. This enhancement in surface functionality is expected to improve the adsorption performance of the biochar.

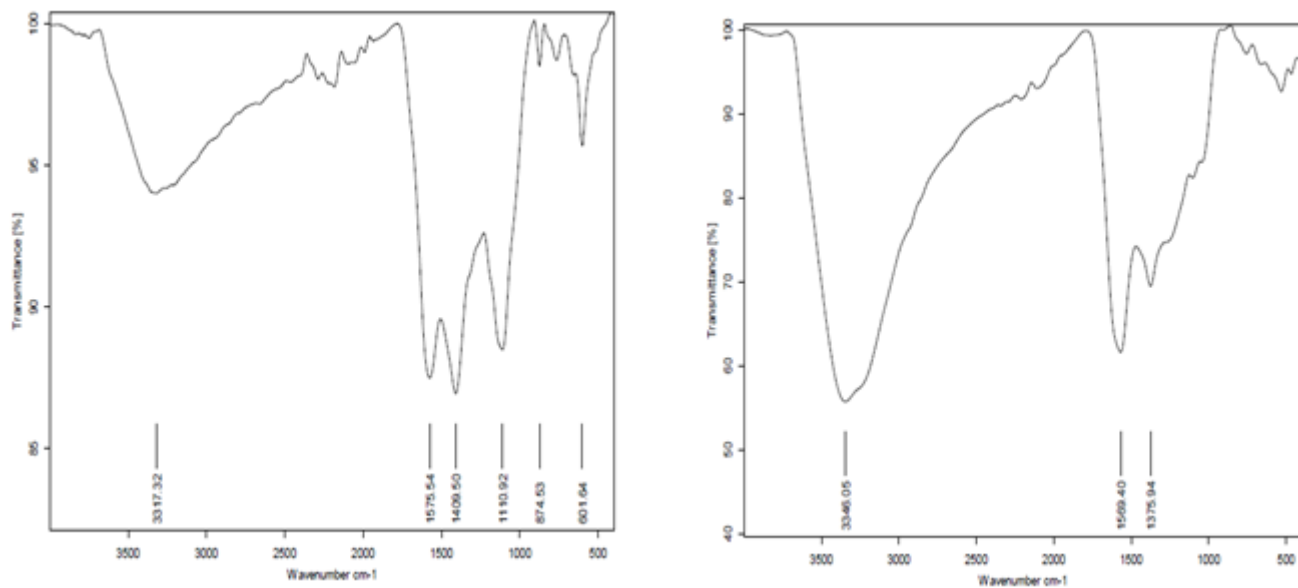


Figure 5. FTIR analysis was performed before and after chemical activation

7.2 SEM Analysis

The surface morphology and structural characteristics of the prepared biochar adsorbent were examined using Scanning Electron Microscopy (SEM). The analysis was performed at an accelerating voltage of 10.0 kV with a magnification of 100 kX and a working distance of 5.2 mm. The obtained micrograph clearly demonstrates a highly irregular and heterogeneous surface morphology with pronounced particle agglomeration. The particles exhibit non-uniform shapes and sizes, forming densely packed clusters. A significantly rough surface texture with well-developed pores and cavities is observed, indicating the presence of a porous network structure. The pore distribution appears uneven, further confirming the heterogeneous nature of the adsorbent surface. The scale bar of 200 nm suggests that the particles predominantly exist in the nanometer range. Such morphological features are indicative of an increased specific surface area and a higher density of active adsorption sites. These characteristics play a crucial role in enhancing the interaction between the adsorbent surface and dye molecules. Consequently, the observed porous and rough surface morphology confirms the suitability of the prepared biochar as an efficient adsorbent for the removal of methylene blue from aqueous media.

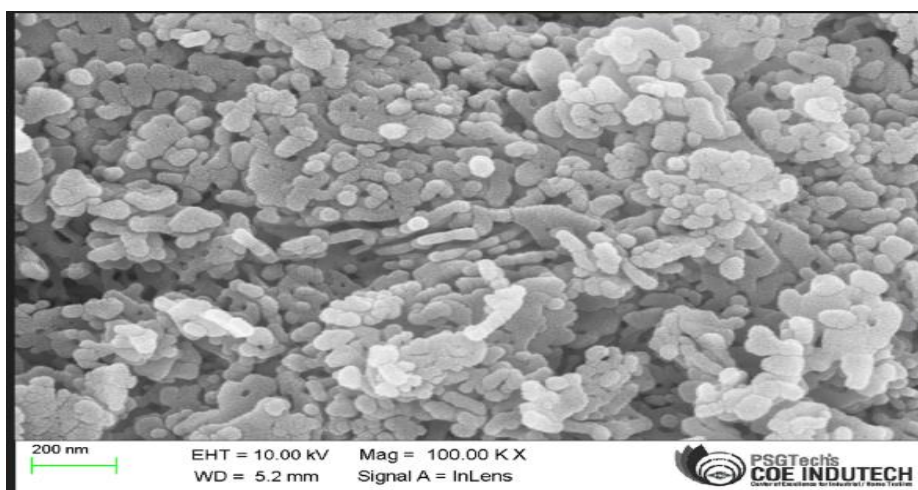


Figure 6. SEM image Chemical activation biochar (KOH)

8. CONCLUSION

Cattail plant biochar shows high potential for removing methylene blue from wastewater, with optimal removal (99.99%) achieved at pH 9, 40-minute contact time, and 0.04 g/100 mL adsorbent dosage. The process follows Freundlich isotherm and pseudo-second-order kinetics, indicating effective multilayer adsorption. This eco-friendly biochar offers a promising solution for dye removal in wastewater treatment.

REFERENCES

- [1] [1] Bacongus, S. R. Abandoned Biomass Resource Statistics in the Philippines. 10th National Convention on Statistics, 2007.
- [2] [2] Obi, F. O., Ugwuishiwu, B. O., & Nwakaire, J. N. Agricultural Waste Concept, Generation, Utilization and Management. Nigerian Journal of Technology 35(4), 2016, pp. 957–964.
- [3] [3] Zhang, C., Song, W., Sun, G., Xie, L., Wang, J., Li, K., Drage, T. CO₂ capture with activated carbon grafted by nitrogenous functional groups. Energy and Fuels 27(8), 2013, pp. 4818–4823.
- [4] [4] Fu, L., Zhang, G., Wang, S., Zhang, L., & Peng, J. Modification of activated carbon via grafting polyethyleneimine to remove amaranth from water. Applied Water Science 7(8), 2017, pp. 4247–4254.
- [5] [5] Bhatnagar, A., & Sillanpää, M. Utilization of agro-industrial and municipal waste materials as potential adsorbents for water treatment-A review. Chemical Engineering Journal 157(2–3), 2010, pp. 277–296.
- [6] [6] Wang, P., Guo, Y., Zhao, C., Yan, J., & Lu, P. Biomass derived wood ash with amine modification for post-combustion CO₂ capture. Applied Energy 201, 2017, pp. 34–44.
- [7] [7] Shoaib, M., & Al-swaidan, H. M. Optimization of activation temperature on the preparation of sliced porous activated carbon from date fronds by physical activation. Hemijiska industrija (Chemical Industry) 70 (2), 2016, pp. 151–15
- [8] [8] Janssen Radley Peñaflores, Airic James Carillo, Samuel Elijah Estrada, Jhulimar Celedonio-Castro. A study on the potential of carbon residue from rice husk used as boiler fuel for carbon dioxide capture and wastewater treatment.